Theory of time-resolved spectral function in high-temperature superconductors with bosonic modes

Jianmin Tao and Jian-Xin Zhu
Theoretical Division & CNLS, Los Alamos National Laboratory, Los Alamos, New Mexico 87545
(Dated: January 4, 2010)

We develop a three-temperature model to simulate the time dependence of electron and phonon temperatures in high-temperature superconductors displaying strong anistropic electron-phonon coupling. This model not only takes the tight-binding band structure into account, but also is valid in superconducting state. Based on this model, we calculate the time-resolved spectral function via the double-time Green's functions. We find that the dip-hump structure evolves with the time delay. More interestingly, new phononic structures are obtained when the phonons are excited by a laser field. This signature may serve as a direct evidence for electron-vibration mode coupling.

PACS numbers: 74.25.Jb, 74.72.-h, 71.38.-k, 79.60.-i

The discovery of high-temperature superconductors (HTSC) has raised an important issue on the mechanism leading to the formation of Cooper pairs, which is still under debate. To address this issue, a number of spectroscopy techniques [1–3] have been used to study the role and nature of bosonic modes, to which electrons are strongly coupled. In particular, due to technological advances and the improved sample quality, angle-resolved photoemission spectroscopy (ARPES) [1] has been used to probe details of the energy and momentum structure of single-particle excitations via the measurement of photoemission intensity. However, different interpretations of the same data may lead to completely different mechanisms [4, 5]. For example, the dip-hump structure observed in ARPES [6–13] could be interpreted [14] as naturnally occurring in the interacting system but having little effect on the superconducting pairing mechanism. It could also be interpreted [15] in terms of phonon modes that could drive d-wave pairing. Recent theoretical analysis [16] on the spectral function of thermally excited electrons in the cuprates has shown that the out-of-plane and out-of-phase buckling mode strongly couples to the electronic states near the anti-nodal M points in the Brillouin zone, while the in-plane breathing mode couples strongly to the electronic states near the d-wave nodal points. The signature of the anistropic electron-phonon (el-ph) coupling seems to get enhanced in the superconducting state, suggesting the significant role of the el-ph interaction in the superconducting mechanism.

The information extracted from the conventional ARPES is limited. Time-resolved ARPES offers the capability to simultaneously capture the single-particle (frequency domain) and collective (time domain) information, thus making it possible to directly probe the link between the collective modes and single-particle states. In this setting, either electrons or lattice vibrational modes can be selectively excited with an ultrafast laser pulse. Recent applications of this technique include the studies of transient electronic structure in Mott insulators [17, 18] and high-T_c cuprates [19] with optical pump. Furthermore, direct pumping of vibrational mode has also been realized in manganites [20], though not yet in the cuprates. Motivated by the thrust of this experimental technique, in this Letter, we aim to provide a theoretical underpinning of transient electronic structure for HTSC, in a hope to better understand the nature of bosonic modes in these systems. As such, the time evolution of the el-ph coupling is investigated for both normal and superconducting states with the time-resolved spectral function. Our theory consists of two parts. First, we develop a three-temperature model to simulate the time dependence of the electron and phonon temperatures. Then, based on the three-temperature model, we calculate the time-resolved spectral function. Our results show a kink-structure in the time dependence of the electronic temperature at the superconducting transition temperature. Accordingly, we find from the spectral density that the energy position of the phonon mode is offset by a time-dependent gap function. More interestingly, new signatures of the el-ph coupling, which are absent when electrons are excited, can be observed in the case of selective excitation of phonons. This signature may serve as a direct evidence for the electron-vibration mode coupling as opposed to the coupling between electrons and spin fluctuations.

Three-temperature model: Consider a two-dimensional superconductor exposed to a laser field. The model Hamiltonian for a vibrational mode ν can be written as

$$\begin{aligned} H &= \sum_{\mathbf{k}\sigma}\xi_{\mathbf{k}}c^{\dagger}_{\mathbf{k}\sigma}c_{\mathbf{k}\sigma}+\sum_{\mathbf{k}}(\Delta_{\mathbf{k}}c^{\dagger}_{\mathbf{k}\uparrow}c^{\dagger}_{-\mathbf{k}\downarrow}+\text{h.c.})+\sum_{\mathbf{q}}\hbar\Omega_{\nu\mathbf{q}} \\ &\times \left(b^{\dagger}_{\nu\mathbf{q}}b_{\nu\mathbf{q}}+\frac{1}{2}\right)+\frac{1}{\sqrt{N_L}}\sum_{\mathbf{kq}\sigma}g_{\nu}(\mathbf{k},\mathbf{q})c^{\dagger}_{\mathbf{k}+\mathbf{q},\sigma}c_{\mathbf{k}\sigma}A_{\nu\mathbf{q}} \\ &+ H_{\text{field}}(\tau), \end{aligned} \tag{1}$$

where $c^{\dagger}_{\mathbf{k}\sigma}$ ($b^{\dagger}_{\nu\mathbf{q}}$) and $c_{\mathbf{k}\sigma}$ ($b_{\nu\mathbf{q}}$) are the creation and annihilation operators for an electron with momentum $\mathbf{k}$ and spin σ (phonon with momentum $\mathbf{q}$ and vibrational mode ν), $A_{\nu\mathbf{q}}=b^{\dagger}_{-\nu\mathbf{q}}+b_{\nu\mathbf{q}}$, the quantity $\xi_{\mathbf{k}}$ is the normal-state energy dispersion, μ the chemical potential, $\Delta_{\mathbf{k}}$ the gap

function, and g_ν the coupling matrix.

By performing the Bogoliubov-de Gennes transformation [21], $c_{\mathbf{k}\uparrow} = u_{\mathbf{k}}\alpha_{\mathbf{k}} - v_{\mathbf{k}}\beta^\dagger_{\mathbf{k}}$ and $c_{-\mathbf{k}\downarrow} = u_{\mathbf{k}}\beta_{\mathbf{k}} + v_{\mathbf{k}}\alpha^\dagger_{\mathbf{k}}$, we obtain $E_e = \sum_{\mathbf{k}} E_{\mathbf{k}}(\langle\alpha^\dagger_{\mathbf{k}}\alpha_{\mathbf{k}}\rangle - \langle\beta_{\mathbf{k}}\beta^\dagger_{\mathbf{k}}\rangle)$, where $E_{\mathbf{k}} = \sqrt{\xi^2_{\mathbf{k}} + \Delta^2_{\mathbf{k}}}$. The time evolution of $\langle\alpha^\dagger_{\mathbf{k}}\alpha_{\mathbf{k}}\rangle$ and $\langle\beta_{\mathbf{k}}\beta^\dagger_{\mathbf{k}}\rangle$ is calculated using the Heisenberg equations-of-motion approach. They are found to be

$$\frac{\partial\langle\alpha^\dagger_{\mathbf{k}}\alpha_{\mathbf{k}}\rangle}{\partial\tau} = \frac{2\pi}{N_L}\sum_{\mathbf{q}} g^2_\nu(u_{\mathbf{k}}u_{\mathbf{k}-\mathbf{q}} - v_{\mathbf{k}}v_{\mathbf{k}-\mathbf{q}})^2(\delta_2 e^{\beta_e\Omega_0} - \delta_1) \times \left[e^{(\beta_{ph}-\beta_e)\Omega_0} - 1\right](1-f_{\mathbf{k}})f_{\mathbf{k}-\mathbf{q}}N_{\Omega_0}\ , \quad (2)$$

and $\partial\langle\beta_{\mathbf{k}}\beta^\dagger_{\mathbf{k}}\rangle/\partial\tau = -\partial\langle\alpha^\dagger_{\mathbf{k}}\alpha_{\mathbf{k}}\rangle/\partial\tau$, where $f_{\mathbf{k}} = f(E_{\mathbf{k}}) = 1/(e^{\beta_e E_{\mathbf{k}}}+1)$, $N_{\Omega_0} = N(\Omega_0) = 1/(e^{\beta_{ph}\Omega_0}-1)$, $\delta_1 = \delta(E_{\mathbf{k}-\mathbf{q}} - E_{\mathbf{k}} + \Omega_0)$, and $\delta_2 = \delta(E_{\mathbf{k}-\mathbf{q}} - E_{\mathbf{k}} - \Omega_0)$. Here we have specifically set $\Omega_\nu = \Omega_0$. Differentiation of both sides of the expression for E_e and substitution of Eq. (2) leads to the rate of energy exchange

$$\frac{\partial E_e}{\partial\tau} = \frac{4\pi}{N_L}\sum_{\mathbf{q}} g^2_\nu(u_{\mathbf{k}}u_{\mathbf{k}-\mathbf{q}} - v_{\mathbf{k}}v_{\mathbf{k}-\mathbf{q}})^2\delta(E_{\mathbf{k}-\mathbf{q}} - E_{\mathbf{k}} - \Omega_0) \times\ \Omega_0\left[e^{(\beta_{ph}-\beta_e)\Omega_0} - 1\right]f_{\mathbf{k}}(1-f_{\mathbf{k}-\mathbf{q}})N_{\Omega_0}\ . \quad (3)$$

Recent experiment [19] shows that there exists cold lattice, which is negligibly coupled to the electrons but dissipates the energy of hot phonons via anharmonic cooling. Considering this observation, we write a set of rate equations for the electron, hot phonon, and lattice temperatures as

$$\frac{\partial T_e}{\partial\tau} = \frac{1}{C_e}\frac{\partial E_e}{\partial\tau} + \frac{P_e}{C_e}, \quad (4)$$

$$\frac{\partial T_{ph}}{\partial\tau} = -\frac{1}{C_{ph}}\frac{\partial E_e}{\partial\tau} + \frac{P_{ph}}{C_{ph}} - \frac{T_{ph}-T_l}{\tau_\beta}, \quad (5)$$

$$\frac{\partial T_l}{\partial\tau} = \left(\frac{C_{ph}}{C_l}\right)\frac{T_{ph}-T_l}{\tau_\beta}, \quad (6)$$

where P_e is the power for pumping electrons and P_{ph} the power for pumping hot phonons. The specific heat of electrons can be calculated from the Boltzmann entropy $S_e = -2k_B\sum_{\mathbf{k}}\{[1-f(E_{\mathbf{k}})]\ln[1-f(E_{\mathbf{k}})] + f(E_{\mathbf{k}})\ln f(E_{\mathbf{k}})\}$ by $C_e = T_e\partial S_e/\partial T_e$, while the specific heat of hot phonons for *one*-vibrational mode can be calculated from the simple relationship $C_{ph} = \hbar\Omega\partial N(\Omega)/\partial T_{ph}|_{\Omega=\Omega_0}$. The results are given by

$$C_e = \beta k_B\sum_{\mathbf{k}}\left(-\frac{\partial f(E_{\mathbf{k}})}{\partial E_{\mathbf{k}}}\right)\left(2E^2_{\mathbf{k}} + \beta\Delta_k\frac{\partial\Delta_k}{\partial\beta}\right), \quad (7)$$

$$C_{ph} = \frac{k_B}{4}\left(\frac{\hbar\Omega_0}{k_BT_{ph}}\right)^2\left[\coth^2\left(\frac{\hbar\Omega_0}{2k_BT_{ph}}\right) - 1\right], \quad (8)$$

respectively, with $\coth x \equiv (e^x + e^{-x})/(e^x - e^{-x})$. Equations (3)-(8) constitute our three-temperature model.

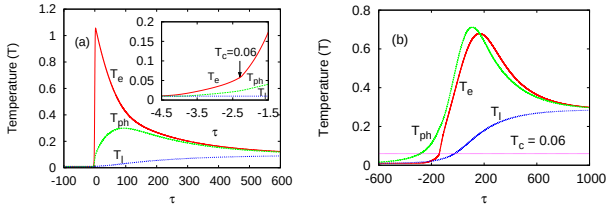

FIG. 1: (Color) Time evolution of electron (T_e), phonon (T_{ph}), and lattice (T_l) temperatures for selectively exciting electrons (a) and phonons (b) with a laser pulse.

The original version of this model was phenomenologically proposed [19] as an extension of the two-temperature model [22] for the normal state. The present model has the following advantages: (i) it incorporates the detailed band structure, (ii) it is valid for *both* normal and superconducting states, and (iii) it includes the anistropic effect on the el-ph coupling.

Now we apply our three-temperature model to simulate the time evolution of the electron, hot phonon, and lattice temperatures for a d-wave superconductor. We use a five-parameter tight-binding model [23] to describe the energy dispersion: $\xi_{\mathbf{k}} = -2t_1(\cos k_x + \cos k_y) - 4t_2\cos k_x\cos k_y - 2t_3(\cos 2k_x + \cos 2k_y) - 4t_4(\cos 2k_x\cos k_y + \cos k_x\cos 2k_y) - 4t_5\cos 2k_x\cos 2k_y - \mu$, where $t_1 = 1$, $t_2 = -0.2749$, $t_3 = 0.0872$, $t_4 = 0.0938$, $t_5 = -0.0857$, and $\mu = -0.8772$. Unless specified explicitly, the energy is measured in units of t_1 and the time is measured in units of $\hbar/t_1$ hereafter. (For $t_1 = 150$ meV, it corresponds to 1740 Kelvin in temperature and $\hbar/t_1$ to 4.4 femtosecond in time.) The d-wave gap function has the form $\Delta_k = \Delta_0(T_e)(\cos k_x - \cos k_y)/2$. The temperature-dependent part is given by [24] $\Delta_0(T_e) = \Delta_{00}\tanh\{(\pi/z)\sqrt{ar(T_c/T_e - 1)}\}$, where $z = \Delta_{00}/(k_BT_c)$ and $\tanh x = 1/\coth x$. In our calculations, we set $\Delta_{00} = 0.2$, the critical temperature $T_c = 0.06$, the specific heat jump at T_c is $r = \Delta C_e/C_e \sim 1.43$, and $a = 2/3$. In this work, we focus on the buckling phonon mode, for which [16, 25, 26] $g_{B_{1g}} = g_0\{[\cos^2(q_x/2) + \cos^2(q_y/2)]/2\}^{-1/2}\{\phi_x(\mathbf{k})\phi_x(\mathbf{k}+\mathbf{q})\cos(q_y/2) - \phi_y(\mathbf{k})\phi_y(\mathbf{k}+\mathbf{q})\cos(q_x/2)\}$ with $\phi_x = (i/N_{\mathbf{k}})[\xi_{\mathbf{k}}t_{x,\mathbf{k}} - t_{xy,\mathbf{k}}t_{y,\mathbf{k}}]$, $\phi_y = (i/N_k)[\xi_{\mathbf{k}}t_{y,\mathbf{k}} - t_{xy,\mathbf{k}}t_{x,\mathbf{k}}]$, $N_{\mathbf{k}} = [(\xi^2_{\mathbf{k}} - t^2_{xy,\mathbf{k}})^2 + (\xi_{\mathbf{k}}t_{x,\mathbf{k}} - t_{xy,\mathbf{k}}t_{y,\mathbf{k}})^2 + (\xi_{\mathbf{k}}t_{y,\mathbf{k}} - t_{xy,\mathbf{k}}t_{x,\mathbf{k}})^2]^{1/2}$, $t_{\alpha,\mathbf{k}} = -2t_1\sin(k_\alpha/2)$, and $t_{xy,\mathbf{k}} = -4t_2\sin(k_x/2)\sin(k_y/2)$. To be consistent with experiment [16, 19], we set $g_0 = 0.4$ and the mode frequency $\Omega_0 = 0.3$. The relaxation time $\tau_\beta = 200$. The pump power is a Gaussian pulse of $P = P_0e^{-\tau^2/(2\sigma^2)}$, for which, the corresponding FWHM (full width at half maximum) is 2.35 σ. To pump electrons, we set $P_0 = 0.15$ and $\sigma = 1$. Considering that the energy scale of phonons is much smaller than that of electrons, we set $P_0 = 0.006$ and $\sigma = 100$ for pumping phonons. The ratio C_{ph}/C_l in Eq. (6) is set to be 0.2.

Figure 1 displays the temporal evolution of three respective temperatures for pumping electrons (a) and hot phonons (b). Before pumping, all three types of degrees of freedom (DoF) are in equilibrium, which is set at $T_e = T_{ph} = T_l = 0.01$. As shown in Fig. 1(a), when the pump pulse is absorbed by the electrons, the electronic temperature rises steeply around $\tau = 0$, and reaches the maximum after a small time delay. It then begins to drop at a time scale determined by the el-ph coupling strength, followed by a slower relaxation. Interestngly, we also observe a small kink in T_e at $T_e = T_c$, which entirely arises from the breakup of the Cooper pairs, resulting in the dramatic change in the rise rate of T_e. This kink was not captured in the early model [19]. Simultaneously, the hot phononic temperature T_{ph} rises smoothly via the energy exchange with electrons and then drops by exchanging energy with the cold lattice, causing the slight increase of T_l. When directly pumping phonons, the time dependence of the temperatures is similarly observed, including the kink in T_e, as shown in Fig. 1(b). Due to the large pumping width, the kink is more easily visible in this case.

Time-resolved spectral function: The time-resolved spectral function is defined as $A(\mathbf{k},\omega) \equiv -\frac{2}{\pi}\,\mathrm{Im}\mathcal{G}_{11}(\mathbf{k},\omega)$. Here $\mathcal{G}_{11}$ is the one-one component of the retarded Green's function $\hat{\mathcal{G}}(\mathbf{k},\omega)$, which is related to the self-energy by $\hat{\mathcal{G}}^{-1}(\mathbf{k},\omega) = \hat{\mathcal{G}}_0^{-1}(\mathbf{k},\omega) - \hat{\Sigma}(\mathbf{k},\omega)$, with $\hat{\mathcal{G}}_0^{-1}(\mathbf{k},\omega) = \omega\hat{\sigma}_0 - \Delta_{\mathbf{k}}\hat{\sigma}_1 - \xi_{\mathbf{k}}\hat{\sigma}_3$. $\hat{\sigma}_{0,1,2,3}$ are the unit and Pauli matrices. As is known [16], in the equilibrium state with $T_e = T_{ph}$, the self-energy can be evaluated more conveniently within the imaginary-time Green's function approach, in which a key step is to convert the Bose-Einstein distribution to the Fermi distribution, $n_B(i\omega_n \pm E_{\mathbf{k}-\mathbf{q}}) = -n_F(\pm E_{\mathbf{k}-\mathbf{q}})$ (with $\omega_n = (2n+1)\pi T$, $T = T_e = T_{ph}$). For the current situation, the temperatures of electrons and hot phonons are no longer tied to each other and the above conversions are not valid any more. To avoid this restriction, here we apply the double-time Green's function approach [27] to calculate $\hat{\Sigma}(\mathbf{k},\omega)$. The result is

$$\begin{aligned}\hat{\Sigma}(\mathbf{k},\omega) &= \frac{1}{N_L}\sum_{\mathbf{q}}|g_\nu(\mathbf{k},-\mathbf{q})|^2 \\ &\{[(\omega-\Omega_0)\Phi_1 - (\omega+\Omega_0)\Phi_2 + \Omega_0(\Phi_3+\Phi_4)]\hat{\sigma}_0 \\ &+[2E_{\mathbf{k}-\mathbf{q}}(\Phi_1-\Phi_3) + 2\Omega_0(\Phi_3-\Phi_4)]\hat{\sigma}_1 \\ &+[\xi_{\mathbf{k}}(\Phi_1-\Phi_2) + (\Omega_0\xi_{\mathbf{k}}/E_{\mathbf{k}})(\Phi_3-\Phi_4)]\hat{\sigma}_3\}, \quad (9)\end{aligned}$$

where $\Phi_1 = N(\Omega_0)/[(\omega-\Omega_0+E_{\mathbf{k}-\mathbf{q}})(\omega-\Omega_0-E_{\mathbf{k}-\mathbf{q}})]$, $\Phi_2 = N(-\Omega_0)/[(\omega+\Omega_0+E_{\mathbf{k}-\mathbf{q}})(\omega+\Omega_0-E_{\mathbf{k}-\mathbf{q}})]$, $\Phi_3 = f(-E_{\mathbf{k}-\mathbf{q}})/[(\omega+\Omega_0-E_{\mathbf{k}-\mathbf{q}})(\omega-\Omega_0-E_{\mathbf{k}-\mathbf{q}})]$, and $\Phi_4 = f(E_{\mathbf{k}-\mathbf{q}})/[(\omega+\Omega_0+E_{\mathbf{k}-\mathbf{q}})(\omega-\Omega_0+E_{\mathbf{k}-\mathbf{q}})]$.

For simplicity, let us first look at the density of states (DOS), which is defined by $\rho(\omega) = \frac{1}{N_L}\sum_{\mathbf{k}} A(\mathbf{k},\omega)$. For direct pumping of electrons, we calculate the DOS at time sequences $\tau = -100$, -2.7, 2.8, and 600, respectively. The results are plotted in Fig. 2 (a). At the initial time

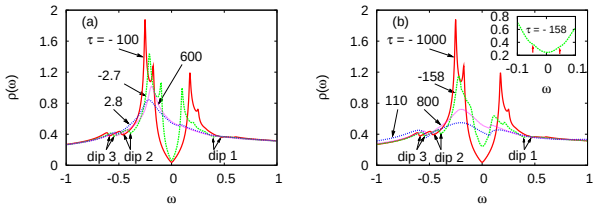

FIG. 2: (Color) Time evolution of the density of states for selectively exciting electrons (a) and phonons (b), respectively.

$\tau = -50$ where $T_e = 0.01$ and the system is at superconducting state [$\Delta_0(T_e) = 0.19$], we observe two signatures of the el-ph coupling located at $\pm(\Omega_0 + \Delta_0(T_e))$, as shown in Fig. 2 (dip 1 and dip 2). They are symmetric with respect to $\omega = 0$, but dip 2 is much stronger. It is related to the fact that the normal-state van Hove singularity is located below the Fermi energy and as such the coherent peak at $-\Delta_0(T_e)$ has stronger intensity than that at $\Delta_0(T_e)$. In addition, dip 3 occurs near the characteristic energy $-(E_M + \Omega_0)$, where E_M is the quasiparticle energy at $\mathbf{k} = (\pi, 0)$ or equivalent wavevector points in Brillouin zone. It arises from the van Hove singularity at $\mathbf{k} = (\pi, 0)$. The signature at the energy $E_M + \Omega_0$ is much weaker also because of the van Hove singularity location in the normal state. At $\tau = -2.7$ where $T_e = 0.041$ and $\Delta_0(T_e) \approx 0.1$, similar behaviors are observed. However, at $\tau = 2.8$, $T_e = 1.05$ and thus only the signature of the normal-state el-ph coupling (dip 3) can be observed. At $\tau = 600$, a similar structure of the normal-state el-ph coupling is observed.

For direct pumping of phonons, we choose different time sequences $\tau = -1000$, -158, 110, and 800 to evaluate the DOS. The results are displayed in Fig. 2(b). From Fig. 2(b), we observe that the dips suggesting the el-ph couplig in both normal and supercondcting states becomes stronger than those for selectively pumping electrons, as expected. In particular, we observe two new small dips at $\omega = \pm 0.05$ for $\tau = -158$ (at which $T_e = 0.041$ and $T_{ph} = 0.163$), both of which arise from the poles of $\Sigma_{\mathbf{k}}(\omega)$ at $\omega = \pm(\Omega_0 - \Delta_0(T_e))$, in addition to those observed in the case of electrons being excited directly. This is because the hot phononic temperature becomes very high while the electronic temperature is still cold and the contributions from the terms as weighted by $N(\pm\Omega_0)$ are significantly enhanced. Figure. 2(b) clearly shows that, as time elapses from $\tau = -1000$, -158, to 110, the peaks move toward the *zero energy*, while from $\tau = 110$ to 800, the locations of these two peaks remain unchanged. This can be understood by considering that, after pumping, T_e rises with the time delay, while $\Delta_0(T_e)$ decreases and rapidly vanishes when T_e reaches T_c.

Finally we numerically evaluate the time-resolved spectral function for the two excitations discussed above at those time sequences chosen for calculating the DOS. In

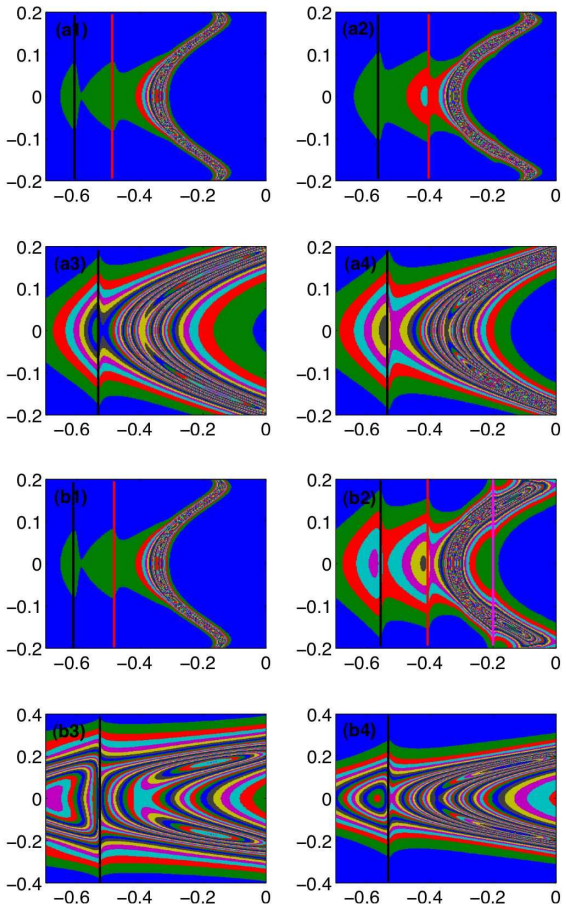

FIG. 3: (Color) Time-resolved spectral function for selectively pumping electrons (a_1-a_4 for $\tau = -100, -2.7, 2.8, 600$) and phonons ($b_1$-$b_4$ for $\tau = -1000, -158, 110, 800$), respectively. The vertical axis is k_x/π at a fixed $k_y = 0.75\pi$ and the horizontal axis is energy. The black, red, and magenta lines represent the energy location, $-(E_M+\Omega_0)$, $-(\Delta_0(T_e)+\Omega_0)$, and $-(\Omega_0 - \Delta_0(T_e))$, corresponding to the dip or hump location discussed in Fig. 2.

our calculations, we consider cuts along k_x-axis in the Brillouin zone at a k_y chosen near the zone boundary. Fig. 3 shows the snapshots of the image of the spectral function $A(\mathbf{k},\omega)$ as a function of k_x and ω. From Fig. 3(a_1,a_2), we observe kinks at $\omega = -(\Delta_0(T_e) + \Omega_0)$ (red lines) and $-(E_M + \Omega_0)$ (black lines) at $\tau = -100$ and -2.7. The red line is shifted in energy as time elapses from $\tau = -100$ to $\tau = -2.7$ because the BCS gap $\Delta_0(T_e)$ drops significantly from 0.19 to 0.1. These kinks correspond to the dip structures discussed in Fig. 2. As $\tau > -2.3$, the superconducting gap vanishes, so do the kinks marked with red lines (see Fig. 3(a_3-a_4)). The kinks marked with black lines persist through the whole time sequence, which can be ascribed to the el-ph coupling signature in the normal state. Therefore we have every reason to regard these kinks marked with red lines as the signature of the el-ph coupling in the superconducting state. For hot phonon pumping (Fig. 3(b_1-b_4)), in addition to those signatures of the el-ph coupling observed for electron pumping, new kink structure at $-(\Omega_0 - \Delta_0(T_e))$(marked with magenta line in Fig. 3(b_2) is also observed. These observations are consistent with our finding in the DOS. In the viewpoint that the electronic spin fluctuations arise from the strong correlation within the electronic DoF itself, and if one can assume that the spin fluctuations will ride on the electrons and thus its effective temperature will be tied to the electronic temperature, direct pumping of hot phonons will provide a unique way to differentiating the bosonic modes being of electronic or phononic origin, to which electronic quasiparticles are strongly coupled in HTSC.

In conclusion, we have developed a three-temperature model to simulate the time evolution of temperature for electrons, hot phonons, and the lattice. Our model takes both quasiparticle excitation and relaxation into account and thus is valid in both normal and superconducting states, because at the early stage of excitation, the system can be still in the supercondcting state. Based on this model, we derive a formula for the time-resolved spectral function, allowing us to investigate the dynamics of the el-ph coupling for HTSC materials.

Acknowledgments. We thank A. V. Balatsky, Elbert E. M. Chia, Hari Dahal, J. K. Freericks, M. Graf, A. Piryatinski, A. J. Taylor, S. A. Trugman, and D. Yarotski for valuable discussions. This work was supported by the National Nuclear Security Administration of the U.S. DOE at LANL under Contract No. DE-AC52-06NA25396, the U.S. DOE Office of Science, and the LDRD Program at LANL.

[1] A. Damascelli, Z. Hussain, and Z.-X. Shen, Rev. Mod. Phys. **75**, 473 (2003).
[2] J. Lee *et al.*, Nature **442**, 546 (2006).
[3] F. Carbone *et al.*, Proc. Natl. Acad. Sci. **105**, 20161 (2008).
[4] M. R. Norman *et al.*, Phys. Rev. B **64**, 184508 (2001).
[5] A. W. Sandvik, D. J. Scalapino, and N. E. Bickers, Phys. Rev. B **69**, 094523 (2004).
[6] H. Ding *et al.*, Phys. Rev. Lett. **76**, 1533 (1996).
[7] J. C. Campuzano *et al.*, Phys. Rev. Lett. **83**, 3709 (1999).
[8] A. Kaminski *et al.*, Phys. Rev. Lett. **86**, 1070 (2001).
[9] A. Lanzara *et al.*, Nature (London) **412**, 510 (2001).
[10] P. D. Johnson *et al.*, Phys. Rev. Lett. **87**, 177007 (2001).
[11] X. J. Zhou *et al.*, Nature (London) **423**, 398 (2003).
[12] T. Sato *et al.*, Phys. Rev. Lett. **91**, 157003 (2003).
[13] T. Cuk *et al.*, Phys. Rev. Lett. **93**, 117003 (2004).
[14] Z. X. Shen and J. R. Schrieffer, Phys. Rev. Lett. **78**, 1771 (1997).
[15] Z.-X. Shen *et al.*, Philos. Mag. B **82**, 1349 (2002).
[16] T.P. Devereaux *et al.*, Phys. Rev. Lett. **93**, 117004 (2004).
[17] L. Perfetti *et al.*, Phys. Rev. Lett. **97**, 067402 (2006).
[18] F. Schmitt *et al.*, Science **321**, 1649 (2008).

[19] L. Perfetti *et al.*, Phys. Rev. Lett. **99**, 197001 (2007).
[20] M. Rini *et al.*, Nature **449**, 72 (2007).
[21] P. G. de Gennes, *Superconductivity of Metals and Alloys* (Benjamin, New York, 1966).
[22] P. B. Allen, Phys. Rev. Lett. **59**, 1460 (1987).
[23] M. R. Norman *et al.*, Phys. Rev. B **52**, 615 (1995).
[24] F. Gross *et al.*, Z. Phys. B **64**, 175 (1986).
[25] J.-X. Zhu *et al.*, Phys. Rev. Lett. **97**, 177001 (2006).
[26] J.-X. Zhu *et al.*, Phys. Rev. B **73**, 014511 (2006).
[27] D. N. Zubarev, Sov. Phys. Usp. **3**, 320 (1960).